Received: 19 April 2020 | Revised: 20 August 2020 | Accepted: 27 August 2020

DOI: 10.1111/cas.14642

ORIGINAL ARTICLE

Cancer Science WILEY

RBPJ contributes to the malignancy of glioblastoma and induction of proneural-mesenchymal transition via IL-6-STAT3 pathway

Guangtao Zhang[1,2] | Shingo Tanaka[1] | Shabierjiang Jiapaer[1] | Hemragul Sabit[1] | Sho Tamai[1] | Masashi Kinoshita[1] | Mitsutoshi Nakada[1]

[1]Department of Neurosurgery, Graduate School of Medical Science, Kanazawa University, Kanazawa, Japan

[2]Division of Life Sciences and Medicine, Department of Neurosurgery, The First Affiliated Hospital of USTC, University of Science and Technology of China, Hefei, China

Correspondence
Shingo Tanaka, Department of Neurosurgery, Graduate School of Medical Science, Kanazawa University, 13-1 Takara-machi, Kanazawa, 920-8641, Japan.
Email: t-shingo@med.kanazawa-u.ac.jp

Mitsutoshi Nakada, Department of Neurosurgery, Graduate School of Medical Science, Kanazawa University, 13-1 Takara-machi, Kanazawa 920-8641, Japan.
Email: mnakada@med.kanazawa-u.ac.jp

Funding information
Kobayashi International Scholarship Foundation; JSPS KAKENHI, Grant/Award Number: 17K10858 and 18H02910; China Scholarship Council

Abstract

Notch signaling plays a pivotal role in many cancers, including glioblastoma (GBM). Recombination signal binding protein for immunoglobulin kappa J region (RBPJ) is a key transcription factor of the Notch signaling pathway. Here, we interrogated the function of RBPJ in GBM. Firstly, RBPJ expression of GBM samples was examined. Then, we knocked down RBPJ expression in 2 GBM cell lines (U251 and T98) and 4 glioblastoma (GBM) stem-like cell lines derived from surgical samples of GBM (KGS01, KGS07, KGS10 and KGS15) to investigate the effect on cell proliferation, invasion, stemness, and tumor formation ability. Expression of possible downstream targets of RBPJ was also assessed. RBPJ was overexpressed in the GBM samples, downregulation of RBPJ reduced cell proliferation and the invasion ability of U251 and T98 cells and cell proliferation ability and stemness of glioblastoma stem-like cells (GSC) lines. These were accompanied by reduced IL-6 expression, reduced activation of STAT3, and inhibited proneural-mesenchymal transition (PMT). Tumor formation and PMT were also impaired by RBPJ knockdown in vivo. In conclusion, RBPJ promotes cell proliferation, invasion, stemness, and tumor initiation ability in GBM cells through enhanced activation of IL-6-STAT3 pathway and PMT, inhibition of RBPJ may constitute a prospective treatment for GBM.

KEYWORDS
glioblastoma, glioblastoma stem-like cells, IL-6, proneural-mesenchymal transition, RBPJ, STAT3

1 | INTRODUCTION

GBM is the most malignant brain tumor in humans. Despite aggressive treatment, including surgical resection, irradiation, and chemotherapy, the overall survival of patients with GBM is typically 14.6-16.0 mo post-diagnosis, and has not improved significantly for decades.[1] The poor prognosis is due not only to the invasiveness and chemo- and radio-resistance of GBM, but also to its cellular heterogeneity.[2,3] Accumulating evidence suggests that GBM is initiated by GSCs, which have the potential to self-renew and are

Abbreviations: DAPI, 4′,6-diamidino-2-phenylindole; GBM, glioblastoma; GFAP, glial fibrillary acidic protein; GSCs, GBM stem-like cells; NB, normal brain tissue; NPCs, neural stem and progenitor cells; PMT, proneural-mesenchymal transition; RBPJ, recombination signal binding protein for immunoglobulin kappa J region; shRNA, small hairpin RNA.

resistant to current therapies.[4-6] Therefore, targeting GSCs could improve the prognosis of GBM. GSCs share some characteristics with neural stem and progenitor cells (NSPCs) such as expression of stem-associated markers, self-renewal, and multilineage differentiation potential.[5,7,8] Signaling pathways that inhibit neuronal differentiation and sustain NSPC populations during development, including Notch, BMP, NF-κB, and Wnt signaling, are also activated in GSCs.[2] Identifying the signaling pathways that drive GSCs is fundamental to understanding the progression of GBM and to developing new treatments.

Notch signaling is highly conserved and plays a key role in the development of many different cell types and tissues, including neurons in the central nervous system.[9,10] Its ligands, receptors, and target genes are frequently overexpressed in cancer tissues and cell lines, such as GSCs, conferring increased tumorigenicity and therapeutic resistance.[11,12] Hence, Notch signaling may be a promising target for new GBM treatments. RBPJ, the chief transcription factor of Notch signaling, is required for all canonical Notch pathways; it also functions beyond Notch signaling.[13-15] RBPJ expression is increased in brain tumors where it may contribute to resistance to anti-Notch drugs.[16,17]

In this study, we evaluated the effect of RBPJ knockdown on the proliferation, invasion, stemness, and tumor initiation ability of 2 glioma cell lines (U251 and T98) and 4 patient-derived GSCs (KGS01, KGS07, KGS10 and KGS15) and investigated the underlying molecular mechanisms.

2 | MATERIALS AND METHODS

2.1 | Surgical specimens

Matched samples of glioma and adjacent non-cancerous brain tissue were collected from patients undergoing resection at the Department of Neurosurgery, Kanazawa University Hospital, with the approval of the human genome/genetic analysis research ethics committee (Approval Number: 209) and the medical ethics committee (Approval Numbers: 2080, 2188) of Kanazawa University. Histological diagnosis of each tumor was based on the World Health Organization (WHO) criteria.[18] Proteins were extracted from fresh-frozen samples for western blotting, while formalin-fixed, paraffin-embedded tissue sections were prepared for immunostaining.

2.2 | Cell culture

HEK293 cells and human GBM cell lines U251 and T98 were purchased from the American Type Culture Collection. The cells were cultured at 37°C in a 5% CO_2 in air incubator, and maintained in Dulbecco's modified Eagle's medium (DMEM) supplemented with 10% heat-inactivated fetal bovine serum (FBS).

To prevent culture-induced drift, patient-derived GSCs were generated from the surgical samples of primary GBM (Figure S1). Cells were cultured in serum-free DMEM/F12 supplemented with B21, 1% GlutaMAX™-I, 20 ng/mL of epidermal growth factor, and 20 ng/mL of b-FGF, as previously described.[19]

2.3 | Vectors and lentiviral transduction

Cells (20×10^4 cells) were seeded into 6-well plates and exposed to 1 of the 2 RBPJ-targeting shRNA lentiviral particles (shRBPJ1, sc270318-v; Santa Cruz Biotechnology; shRBPJ2, Sigma-Aldrich) or non-targeting control (sc108080; Santa Cruz Biotechnology) shRNA lentiviral particles. After 3 d of incubation, puromycin dihydrochloride (sc-108071, Santa Cruz Biotechnology) was used to select stably transduced cells. Puromycin selection was applied for at least 72 h, and RBPJ knockdown was verified by western blotting. RBPJ-silenced (shRBPJ1 and shRBPJ2) and control (shCONT) cells were expanded for subsequent experiments.

2.4 | Western blotting

Cells and surgical specimens were lysed in a lysis buffer (Sigma-Aldrich) containing a mixture of protease and phosphatase inhibitors (Sigma-Aldrich). Then, cellular proteins were extracted and cleared by centrifugation (20 600 *g*) at 4°C for 10 min. The samples were analyzed for the proteins of interest using standard western blotting techniques,[20] using antibodies against RBPJ, phosphorylated STAT3 (Y705), total STAT3, CD44, PDGFRα (Cell Signaling Technology), IL-6 (Abcam), CD133 (R&D Systems), GFAP (Dako), YKL-40 (Quidel Corporation), OLIG2 (IBL), and SOX2 (GeneTex).

2.5 | Immunohistochemistry

Paraffin-embedded glioma samples were cut into 4-μm thick sections. Samples were deparaffinized in xylene, rehydrated, then autoclaved in TRS (pH 6.0) at 120°C for 10 min to retrieve antigens. Endogenous peroxidase activity was blocked by treatment with 3% hydrogen peroxide in methanol for 20 min. Subsequently, the sections were blocked with 5% skimmed milk in TBS-T for 30 min, and then incubated overnight at 4°C with the primary antibodies. The next day, the sections were washed with TBS-T 3 times and incubated for 1 h at room temperature using an Envision + kit (Dako, K4001) for secondary antibody. The reaction was visualized with 3,3′-diaminobenzidine tetrahydrochloride for 5 min before the sections were counterstained with hematoxylin. Antibodies against the following antigens were used: RBPJ, PDGFRα, CD44 (Cell Signaling Technology), Ki-67 (Thermo Scientific), YKL-40 (Quidel Corporation), and OLIG2 (IBL).

2.6 | Immunofluorescence

The tissue sections were treated as for immunohistochemistry. For cells, coverslips were coated with 30-50 μL of laminin (50 μg/mL) to

allow the cells to adhere as uniform monolayers. Subsequently, the cells were fixed in 4% paraformaldehyde for 15 min, permeabilized, blocked in 5% skimmed milk in TBS-T, and incubated overnight with antibodies against the following antigens: RBPJ, CD44 (Cell Signaling Technology), CD133, TUJ-1 (R&D Systems), SOX2 (Gene Tex), GFAP (Dako), and OLIG2 (IBL).

After incubation with the primary antibodies, the tissue sections and coverslips were probed with a fluorescent anti-rabbit antibody or a fluorescent anti-mouse antibody for 1 h at room temperature in the dark. Finally, the sections were mounted using a mounting medium containing DAPI (Santa Cruz Biotechnology). Images were acquired using a BZ-X700 microscope (Keyence) and digitally processed with Keyence analysis software (Keyence).

2.7 | Cell proliferation assay

Alamar blue assay (Biosource) or CCK-8 assay (Dojindo) was performed to measure cell proliferation. For the Alamar blue assay, cells treated with different shRNAs or drugs were seeded into 96-well plates at a density of 1×10^3 cells/well. Alamar blue solution (20 μL) was added to each well before the plate was read on a microplate reader (measurement, 590 nm; reference, 540 nm) at 0, 24, 48, 72, and 96 h (or longer if the cells grew slowly). Absorbance values from 6 wells were averaged and plotted. For the CCK-8 assay, cells were seeded at a density of 5×10^3 cells/well and the absorbance at 450 nm was measured 4 h after CCK-8 was added to each cell every 24 h for 3 d.

2.8 | Invasion assay

Invasion assay was performed using the transwell system with a Matrigel-coated membrane, as previously described.[19] Migrated cells were counted in 6 random high-powered fields.

2.9 | Sphere-forming assay

Sphere-forming assay was performed to evaluate the stemness of each GSC line, as previously described.[21] Briefly, GSC spheres were dissociated into single cells using StemPro Accutase (Gibco/Life Technologies). Then, 1×10^3 single cells were seeded into a 96-well Costar ultra-low attachment plate (Corning) in 200 μL neurosphere medium supplemented with 1.0% methylcellulose. After 7 d of incubation, the tumor spheres with a diameter larger than 50 μm were counted.

2.10 | Intracranial tumor formation in vivo

To evaluate tumor initiation ability of GSCs, we carried out animal experiments, as described previously.[22] Healthy female nude mice (BALB/cSlc-nu/nu, Charles River Laboratories) aged 4-5 wk were obtained and maintained in a pathogen-free facility at the Institute for Experimental Animals of Kanazawa University. Mice were housed in a temperature-controlled room with a 12-h : 12-h, light : dark cycle, and provided free access to water. For the xenograft experiments, mice were randomly divided into 2 groups (4 per group). Viable GSCs (1×10^4/animal) that were transduced with shCONT or shRBPJ1 were engrafted intracranially into the brains of nude mice that were anesthetized using 5% pentobarbital sodium (Koritsu Seiyaku Corporation). The experiment was repeated 2 times to evaluated survival and tumor growth respectively. For the survival experiments, the animals were maintained until manifestation of neurological symptoms, or for 150 d. To assess tumor growth, mouse brains implanted with GSCs expressing shRBPJ1 or shCONT were harvested on day 50 after GSC implantation. Animals were anesthetized using 5% pentobarbital sodium before they were euthanized via cervical dislocation, then brains were collected. The brain tissues were dissected, embedded in paraffin, and then cut into 4-μm serial coronal sections for H&E staining, immunohistochemical staining, and immunofluorescent staining. The project was approved by Institute for Experimental Animals of Kanazawa University advanced research center (approval numbers: 163758, 163761), and all animal experiments were carried out in accordance with the Guidelines for the Care and Use of Laboratory Animals at Kanazawa University that covers the national guideline.

2.11 | Statistical analyses

All grouped data were presented as mean ± standard deviation (SD). For the proliferation assay, repeated-measures ANOVA was used to compare the groups. For other in vitro assays, differences between groups were assessed by one-way ANOVA. All in vitro experiments were repeated at least 3 times. For the in vivo experiments, log-rank survival analysis was performed. *P*-values < .05 were considered to indicate statistically significant differences. SPSS software (version 20) was used for all statistical analyses.

2.12 | Ethics approval and consent to participate

Approval: All experimental protocols including animal experiments were approved by the human genome/genetic analysis research ethics committee (Approval Number: 209), the medical ethics committee (Approval Numbers: 2080, 2188), and Institute for Experimental Animals of Kanazawa University (Approval Numbers: 163758, 163761). Accordance: All methods including animal experiments were carried out in accordance with relevant guidelines and regulations. Informed consent: Written informed consent was obtained from all participants or their representative related to this research.

3 | RESULTS

3.1 | RBPJ is differentially expressed in GBM and non-tumor brain tissue

Western blotting of proteins extracted from surgical specimens of GBM and paired non-tumor brain tissue showed that RBPJ was overexpressed in tumor tissue (Figure 1A). All GBM samples displayed high levels of the protein, and 1 case of WHO grade III glioma had low RBPJ levels; RBPJ expression was not observed in WHO grade II glioma (Figure 1B). Moreover, immunohistochemical staining showed that RBPJ expression was derived from GBM cells in the nucleus, while normal brain cells did not express the protein (Figure 1C and Figure S2).

3.2 | RBPJ knockdown suppresses proliferation and invasiveness of GBM cell lines

Expression of RBPJ in U251 and T98 cells was confirmed by western blotting, with HEK-293 cells acting as a positive control (Figure 2A).[23] To assess the function of RBPJ in GBM cells, we knocked down its expression in U251 and T98 cells using lentiviral shRNA constructs (Figure 2B). Downregulation of RBPJ levels decreased proliferation (Figure 2C) and significantly suppressed invasiveness of both cell lines (Figure 2D).

3.3 | RBPJ downregulation suppresses proliferation and stemness of GSCs

As Notch signaling is important for maintaining stemness of GSCs,[2,21,24] RBPJ, as the cardinal transcription factor of the Notch signaling pathway, may be instrumental for proper GSC function. To investigate this, we first confirmed that RBPJ was expressed in GSCs (Figure 3A). Next, we examined RBPJ levels in matched samples of GSCs and FBS-differentiated GBM cells to determine whether RBPJ could be a stem-associated marker. In each matched set, GSCs displayed higher RBPJ levels than differentiated GBM cells (Figure 3B). Differentiation was confirmed by detection of CD133 (a stem-associated maker) and GFAP (a differentiation marker). As RBPJ is preferentially expressed in GSCs, we used GSC

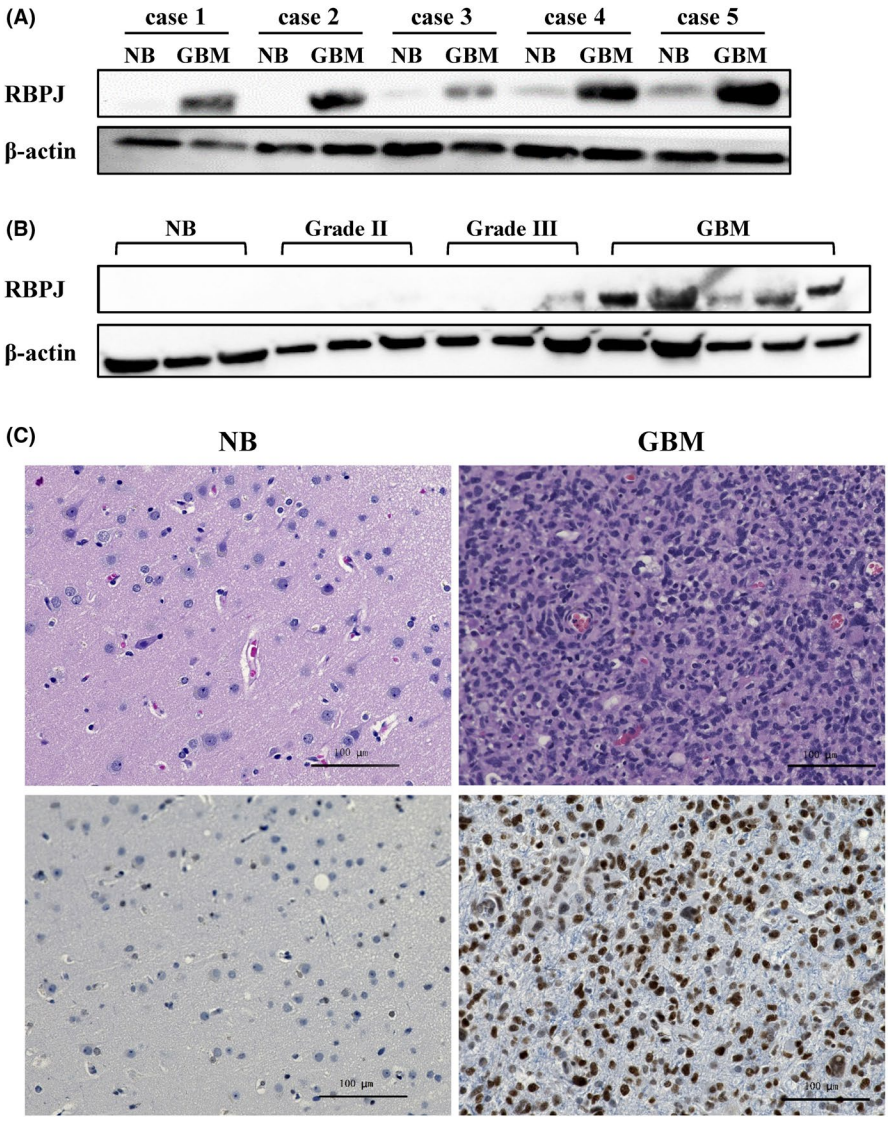

FIGURE 1 RBPJ expression in surgical glioblastoma (GBM) specimens. A, RBPJ levels in GBM tissue and paired normal brain tissue (NB), as assessed by western blotting. β-Actin was used as a loading control. B, RBPJ expression in gliomas of different WHO grades. C, Hematoxylin and eosin staining and immunohistochemistry of RBPJ in surgical specimens of GBM and NB. Scale bars, 100 μm

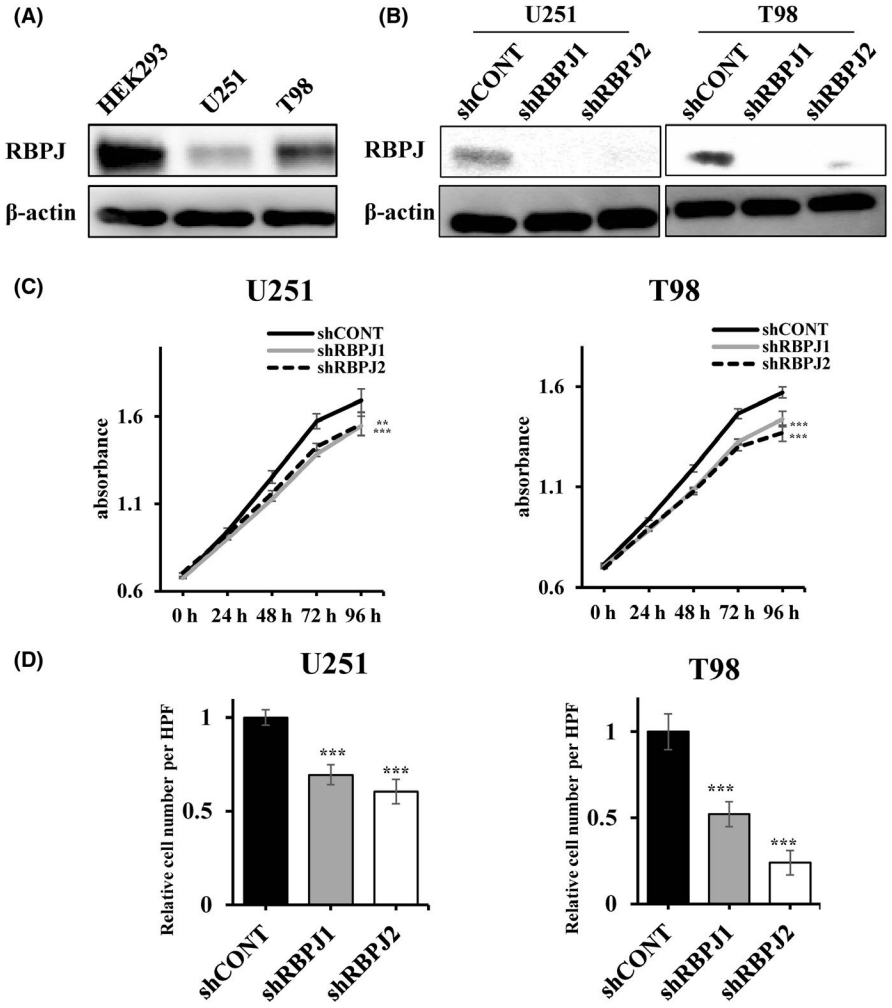

FIGURE 2 Effects of RBPJ knockdown on the proliferation and invasiveness of glioblastoma (GBM) cells. A, Expression of RBPJ in 2 GBM cell lines (U251 and T98), as evaluated by western blotting. HEK293 cells served as a positive control for RBPJ expression. B, Decreased RBPJ protein level in cells transduced with both RBPJ-targeting small hairpin RNA (shRNA)1 and 2 compared with the control in GBM cells. C, Proliferation assay using Alamar blue. Both shRBPJ1 and 2 suppressed proliferation ability of GBM cells. Data are presented as the mean ± standard deviation (SD) (n = 6). *$P < .05$; ** $P < .01$, ***$P < .001$. D, Invasiveness of RBPJ-silenced and control GBM cells, as assessed by transwell assay. Invasiveness of RBPJ-silenced GBM cells was reduced compared with that of control cells. The bars represent mean cell counts from at least 6 high-powered fields (HPF). *$P < .05$; ** $P < .01$, ***$P < .001$

lines to examine whether RBPJ played a role in their proliferation and stemness maintenance. RBPJ was successfully knocked down in all the 4 GSC lines used (Figure 3C). Cells transduced with both shRBPJ1 and shRBPJ2 proliferated at a lower rate than those transduced with shCONT (Figure 3D). To assess the effect of RBPJ on self-renewal, the main characteristic of stem-like cells, we performed the sphere-forming assay. GSCs transduced with shRBPJ1 and shRBPJ2 formed fewer neurospheres than control cells (Figure 3E and Figure S3).

3.4 | RBPJ knockdown inhibits the activation of STAT3

To elucidate the molecular mechanisms mediating the above effects, we studied changes in expression of downstream targets of RBPJ that may be related to proliferation, invasiveness, or stemness of cancer cells such as HES1, p-AKT/AKT, p-ERK/ERK, p-STAT3/STAT3, and p-mTOR. Among the proteins we investigated, the level of phosphorylated STAT3 (p-STAT3 [Y705]) was decreased after RBPJ knockdown in all GBM cell lines and GSC lines used, whereas the expression of total STAT3 remained unaltered (Figure 4A). It is reasonable to speculate that RBPJ did not regulate STAT3 expression directly as a transcription factor, rather it regulates STAT3 activation through other factors. Excessive STAT3 activation occurs in response to cytokines, including IL-6,[25] therefore we assessed IL-6 expression using western blotting. IL-6 levels were reduced by RBPJ knockdown, suggesting that RBPJ influenced STAT3 activation through IL-6 (Figure 4A). To confirm if IL-6 was a main cause of STAT3 activation, we treated the cells with a neutralizing antibody targeting IL-6 (Abcam). STAT3 activation was evaluated using western blotting 72 h after administration of the antibody. The result showed that blockade of IL-6 caused decreased STAT3 activation, as shown by the level of phosphorylated STAT3 (Y705) (Figure 4B). Rescue experiments were also performed using recombinant human IL-6 (Oriental Yeast Company, Japan). Decreased proliferation, invasion, and sphere-forming ability of the cells caused by RBPJ knockdown were rescued by IL-6 administration (Figure S6). Furthermore, the inhibitory effect of RBPJ knockdown on STAT3 activation was attenuated by IL-6 administration (Figure S7A).

3.5 | RBPJ is related to PMT

To explain the effect of RBPJ knockdown on stemness maintenance of GSCs, we assessed the expression of putative stem-associated

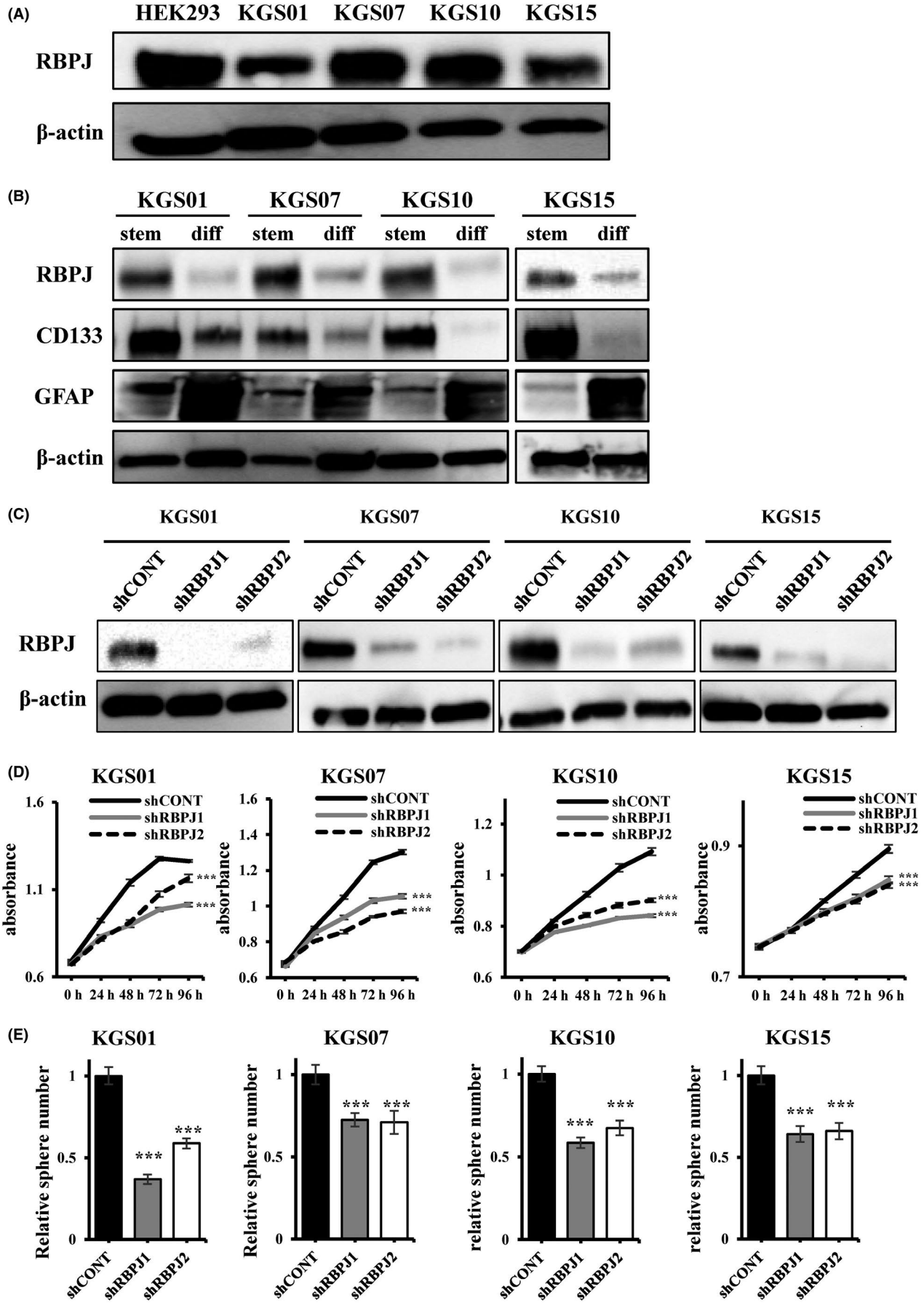
(A)
HEK293 KGS01 KGS07 KGS10 KGS15
RBPJ
β-actin
(B)
KGS01 KGS07 KGS10 KGS15
stem diff stem diff stem diff stem diff
RBPJ
CD133
GFAP
β-actin
(C)
KGS01 KGS07 KGS10 KGS15
shCONT shRBPJ1 shRBPJ2
RBPJ
β-actin
(D)
KGS01 KGS07 KGS10 KGS15
shCONT
shRBPJ1
shRBPJ2
absorbance
0 h 24 h 48 h 72 h 96 h
***
(E)
KGS01 KGS07 KGS10 KGS15
Relative sphere number
relative sphere number
shCONT shRBPJ1 shRBPJ2
***

FIGURE 3 RBPJ expression in glioblastoma stem-like cells (GSCs) and the effect of RBPJ knockdown on the proliferation and self-renewal of GSCs. A, RBPJ expression in GSC lines, as assessed by western blotting. HEK293 cells served as a positive control for RBPJ expression. B, RBPJ expression in GSCs and FBS-differentiated GBM cells derived from the same patients. RBPJ protein expression of all GSCs we used were significantly higher compared with FBS-differentiated GBM cells. Stemness and differentiation were confirmed by positive CD133 and glial fibrillary acidic protein (GFAP) staining, respectively. C, RBPJ protein levels in cells transduced with control and RBPJ-targeting shRNAs, as examined by western blotting. RBPJ protein level was decreased in cells transduced with both shRBPJ1 and shRBPJ2 compared with control for all GSCs. D, Proliferation assay using Alamar blue. RBPJ suppression inhibited the proliferation of all GSCs. Data are presented as means ± SD (n = 4). *$P < .05$; ** $P < .01$, ***$P < .001$. E, Effects of RBPJ knockdown on GSC tumorsphere formation. Numbers of tumor spheres formed by both shRBPJ1 and shRBPJ2 cells were decreased compared with shCONT cells. Data are presented as means ± SD (n = 3). *$P < .05$; ** $P < .01$, ***$P < .001$

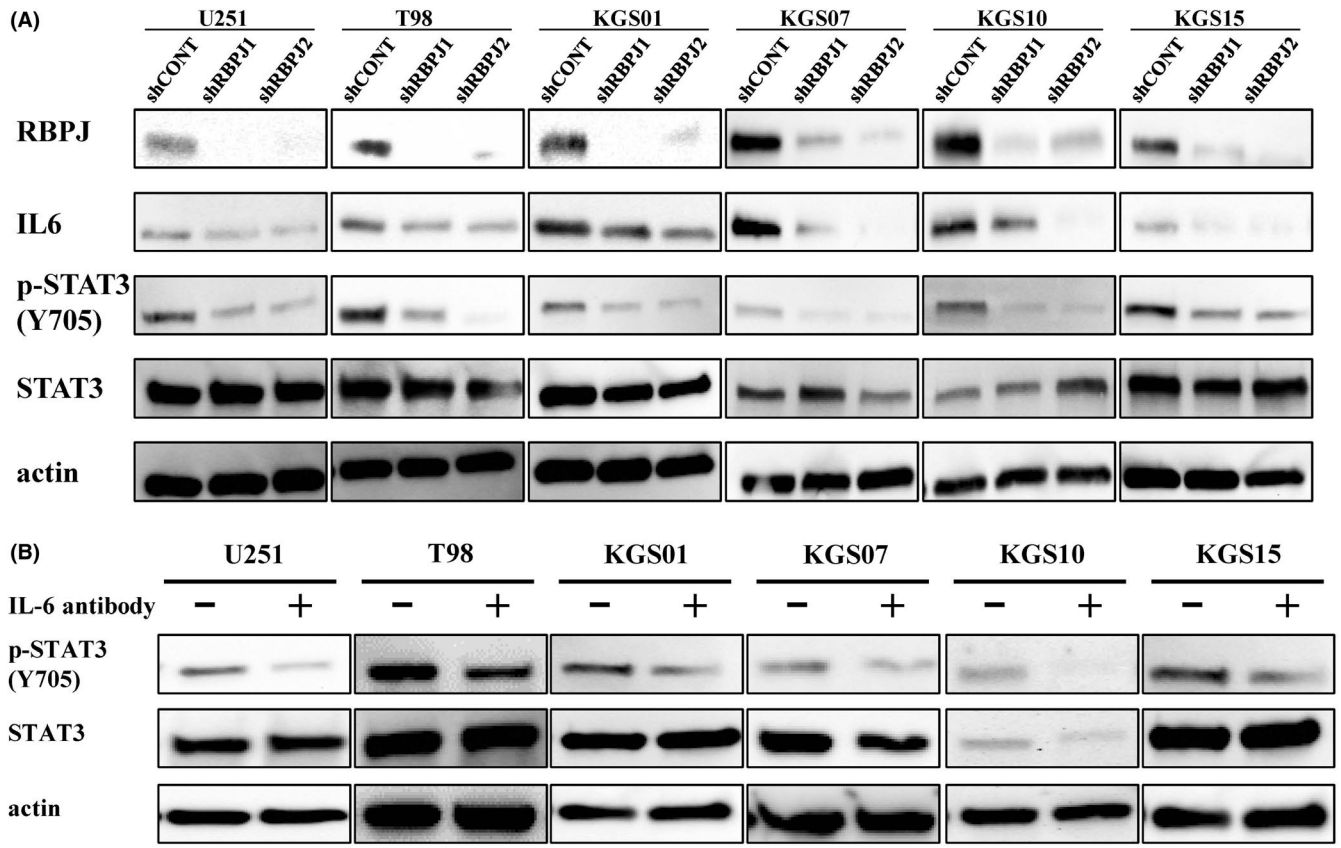

FIGURE 4 RBPJ regulated IL-6 and phosphorylated STAT3. A, Protein levels of IL-6 and p-STAT3 (Y705) after RBPJ knockdown. Protein levels of both IL-6 and p-STAT3 (Y705) were decreased in glioblastoma (GBM) cell lines and GBM stem-like cells (GSCs) transduced with both shRBPJ1 and shRBPJ2 compared with control cells. B, The protein level of p-STAT3 (Y705) in cells treated with a neutralizing antibody targeting IL-6. p-STAT3 (Y705) was decreased with the administration of the neutralizing IL-6 antibody in all GBM cell lines and GSCs

markers CD133 and SOX2 using western blotting. Levels of neither marker were significantly altered (Figure S5). Interestingly, expression of the mesenchymal marker CD44[26,27] was decreased in both the 2 GSC lines that expressed it (KGS01and KGS15), while that of the proneural marker OLIG2[26] was increased in all GSC lines used (Figure 5). These findings led us to hypothesize that RBPJ promotes PMT. Further, we observed the expression of YKL-40[26] (mesenchymal marker) and PDGFRα[27] (proneural marker). As expected, YKL-40 was downregulated in all 4 cell lines. Notably, PDGFRα was upregulated in all cell lines used (Figure 5). This could be reversed by administration of IL-6, indicating that RBPJ regulated PMT at least partially through IL-6 (Figure S7B).

3.6 | Targeting RBPJ suppresses GSC growth and increases survival of mice bearing intracranial GBM xenografts

The most important property of GSCs is their ability to induce the reappearance of tumors in xenografts, even in low numbers. As RBPJ is required for maintaining the tumorigenic potential of GSCs, we investigated whether RBPJ knockdown could affect the growth of GSC-initiated tumors in vivo. GSCs transduced with shRBPJ1 or shCONT were transplanted into brains of nude mice (4 mice for each group); RBPJ expression in shRBPJ1-transduced cells was confirmed by immunofluorescence (Figures 6A and S9A).

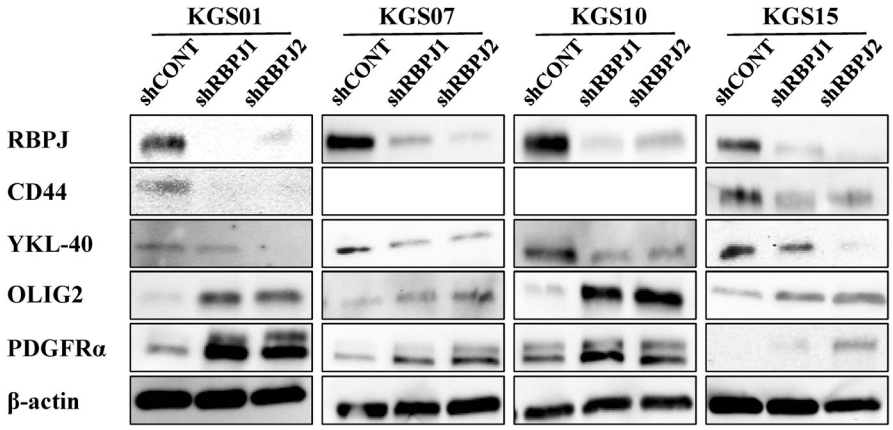

FIGURE 5 RBPJ may be related to proneural-mesenchymal transition (PMT). RBPJ knockdown decreased CD44 expression of the 2 cell lines that originally expressed it (KGS01 and KGS15). Similarly, YKL-40 expression was decreased in all glioblastoma stem-like cells (GSCs) by RBPJ suppression. RBPJ suppression increased OLIG2 and PDGFRα expression of all GSCs. These results suggested that RBPJ is involved in PMT

Ki-67 staining was performed to reveal the tumor area (Figures 6A and S9A). Animals bearing shRBPJ1-expressing GSCs displayed reduced tumor formation (Figures 6A and S9A) and longer overall survival (Figures 6B and S9B) compared with those bearing shCONT-expressing cells. YKL-40 levels were lower, while those of OLIG2 were higher in tumors formed by KGS10 shRBPJ1 cells than in those derived from KGS10 shCONT cells (Figure 6C). CD44 was not expressed in KGS10 cells originally and the level of PDGFRα did not differ between the 2 groups (Figure 6C). In mice transplanted with KGS01 cells, CD44 expression was significantly lower, and that of OLIG2 was higher in tumors formed by shRBPJ1 cells (Figure S9C). This indicated that PMT was also inhibited in vivo after RBPJ knockdown.

4 | DISCUSSION

Our data showed that RBPJ was more highly expressed in GBM than in normal brain tissue or low-grade gliomas, and that it promoted cell proliferation, invasion, and stemness maintenance in GBM cells. Interestingly, RBPJ levels were markedly higher in GSCs than in differentiated GBM cells, suggesting that RBPJ could be used as a stem-associated marker along with CD133. RBPJ promoted GBM progression in vitro through activation of the IL-6/STAT3 pathway and induction of PMT. RBPJ knockdown also suppressed PMT in vivo, attenuating tumor progression. This study is the first to show that RBPJ activates STAT3 and PMT in GBM cells.

Multiple factors contribute to the malignancy of glioma such as mutation of oncogenes or tumor suppressors and dysregulation of signaling pathways, metabolism, or the tumor microenvironment.[28,29] We showed that RBPJ expression was higher in GBM tissues than in healthy brain tissues or low-grade gliomas. Thus, RBPJ concentration appeared to be correlated with the degree of glioma malignancy. A previous report based on The Cancer Genome Atlas (TCGA) data concluded that RBPJ mRNA was expressed at a higher level in GBM than in healthy brain, and that upregulation of RBPJ might be associated with poor prognosis in GBM.[30] Our in vivo findings supported the potential role of RBPJ as a prognostic marker for GBM. Notably, another report utilizing TCGA data showed that RBPJ mRNA levels were not always higher in GBM than in WHO grade I-III gliomas,[31] and was in contrast with our observations. The cause of this discrepancy may be that mRNA and protein levels do not always match.[32] Our study was in accordance with a previous study that compared RBPJ protein expression in gliomas and healthy brain tissue.[33] Based on our data, we propose that RBPJ levels are strongly related to glioma malignancy and that RBPJ is a promising molecular target for GBM.

RBPJ regulates self-renewal and proliferation of cancer stem-like cells in solid tumors, including GBM.[30,31] However, there have only been 2 reports on RBPJ in GSCs.[30,31] Here, RBPJ knockdown inhibited stemness and decreased cell proliferation in all 4 patient-derived GSC lines, which was in line with previous reports. Our results supported the idea that GSC function is regulated by RBPJ. Moreover, we showed that differentiated GSCs had lower levels of RBPJ and CD133, and higher levels of GFAP than undifferentiated cells. CD133 is a putative cell surface marker for cancer stem-like cells whose validity remains controversial.[34] In our study, in some GSC lines, RBPJ expression was reduced to a higher extent than that of CD133. This suggests that, in GBM, RBPJ is a more robust stem-associated marker than CD133. A previous study identified GSCs with activated Notch signaling ($Notch^{hi}$ GSCs), and those GSCs with high CD133 expression ($CD133^{hi}$ GSCs), such as heterogeneous populations in GBM. $Notch^{hi}$ GSCs have the potential to generate $CD133^{hi}$ lineages, but the inverse is not possible, and $Notch^{hi}$ GSCs can regulate microvascular niches in GBM.[35] As RBPJ is strongly associated with the activation of Notch signaling,[35] targeting RBPJ may be a viable approach for the elimination of GSCs.

RBPJ knockdown reduced STAT3 phosphorylation in all cell lines used in this study. STAT3 signaling promotes self-renewal and proliferation of GSCs, and regulates the tumor immune-environment in GBM.[36,37] Therefore, STAT3 in GSCs is a potential molecular target for treatment of GBM.[19,38,39] Stemness maintenance and cell proliferation were impaired by RBPJ suppression through diminished STAT3 phosphorylation. We also administered DAPT, an inhibitor of Notch, to all cell lines. The results showed that GBM cells treated with DAPT had decreased proliferation, invasion, and sphere-forming ability compared with cells with RBPJ knockdown (Figure S8A-D). The expression level of p-STAT3 (Y705) was decreased in all

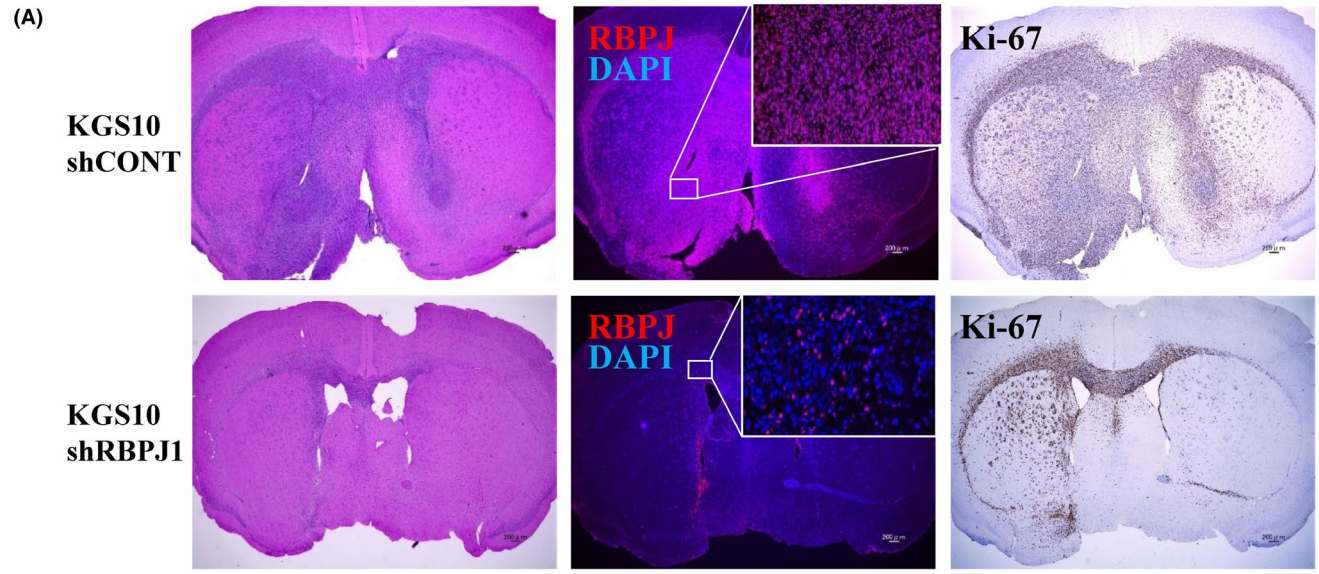

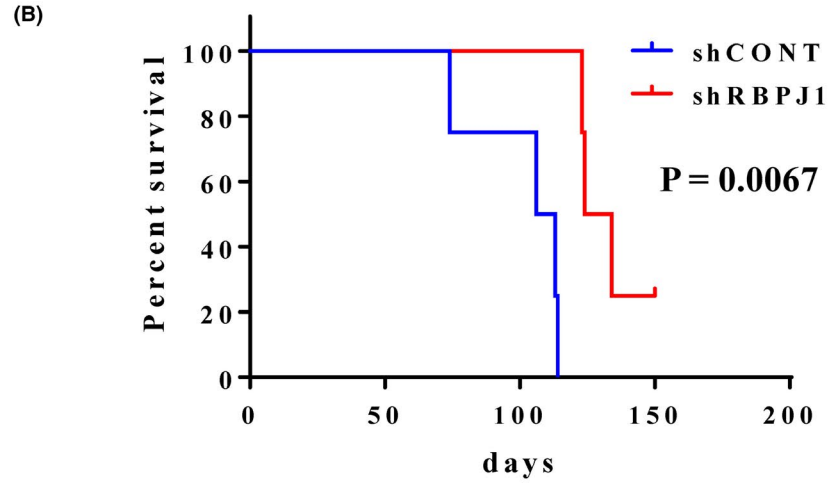

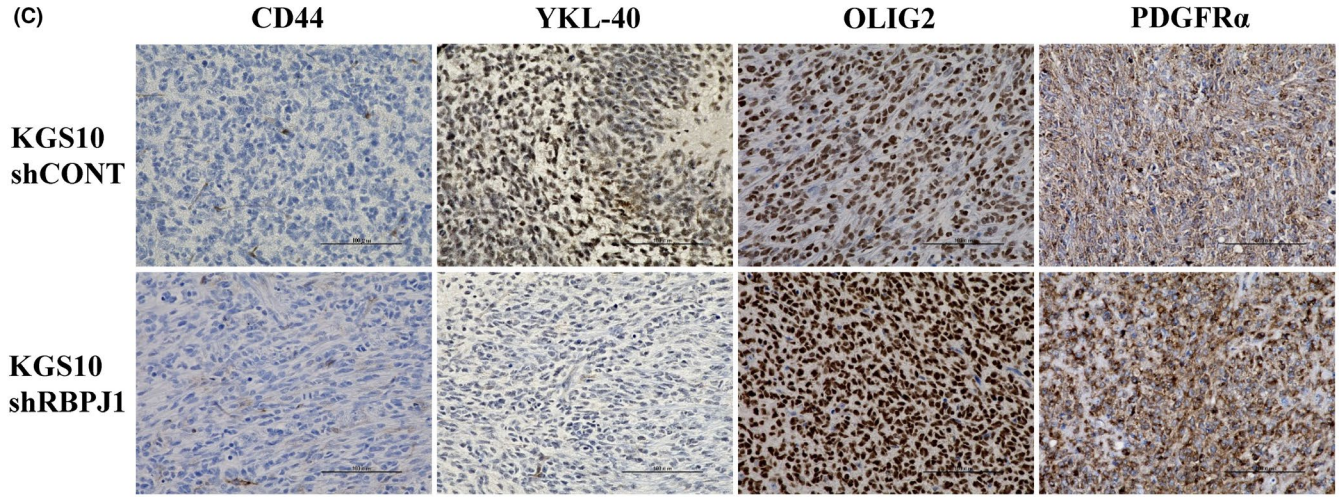

FIGURE 6 RBPJ knockdown in glioblastoma stem-like cells (GSCs) suppressed tumor growth and increased survival of animals bearing intracranial GBM. A, Hematoxylin and eosin staining, immunofluorescence staining of RBPJ and immunohistochemistry of Ki-67 for mouse brain tissue implanted with KGS10-shRBPJ1 or KGS10-shCONT. The tumor area of KGS10-shRBPJ1 was clearly smaller than that of the control. Scale bars, 200 μm. B, The Kaplan-Meier curve of KGS10-shRBPJ1 group and shCONT group. The survival time of KGS10-shRBPJ1 group was significantly longer than that of KGS10-shCONT. C, Immunohistochemical staining showing the expression of CD44, YKL-40, OLIG2 and PDGFRα. Expression of YKL-40 was decreased, while that of OLIG2 was increased in tumors formed by KGS10-shRBPJ1 cells. CD44 was not originally expressed in KGS10 cells and the levels of PDGFRα were not significantly changed. Scale bars, 100 μm

GBM cells treated with DAPT (Figure S8E). The effects of DAPT treatment on GBM cells were similar to that of RBPJ knockdown. This indicated that the effects of RBPJ suppression might be at least partially Notch-dependent. RBPJ is a nuclear protein that transduces the activity of Notch signaling.[13,14] Therefore, targeting RBPJ may be a useful strategy for eliminating GSCs.

STAT3 is activated by IL-6 signaling in GBM,[25] where it is implicated in cell invasion, tumor progression, and resistance to radio- and chemotherapy.[40,41] Protein levels of both IL-6 and phosphorylated STAT3 were decreased in all RBPJ-silenced GBM cell lines we used. Further, RBPJ regulated IL-6 transcription by binding to the promoter region of the *IL-6* gene in some cells of the immune system.[42-44] ChIP-seq data (GSM1922946 and GSM1922947)[45] obtained from the Cistrome database (http://cistrome.org/) also demonstrated a binding site of RBPJ on the promoter region of the *IL-6* gene (Figure S4). This provided the clue that RBPJ may regulate expression of *IL-6* directly as a transcriptional factor. Blockade of IL-6 caused STAT3 dephosphorylation, this finding was consistent with that of a previous study.[46] Additionally, IL-6 administration could rescue the inhibitory effect on STAT3 activation caused by RBPJ knockdown, suggesting that RBPJ could regulate activation of STAT3, at least in part through the autocrine effect of IL-6. Taken together, these findings suggested that a RBPJ-IL-6-STAT3 axis exists in GBM cells. To our knowledge, the current study is the first to propose the existence of an RBPJ-IL-6-STAT3 axis and implicate it in tumor progression and stemness maintenance of GSCs.

Glioblastomas were classified by genetic background into 4 subtypes, such as proneural, neural, classical, and mesenchymal subtypes.[47] Among these subtypes, the mesenchymal subtype is the most aggressive and strongly associated with a poor prognosis.[48] While GSCs are mainly divided into proneural-like GSCs and mesenchymal-like GSCs based on genetic and molecular signatures.[49-51] It has been reported that there is a transition of phenotypes in GSCs caused by tumor microenvironment and radiotherapy.[51] Here, we demonstrated that RBPJ suppression is related to upregulation of proneural markers and downregulation of mesenchymal markers, indicating that RBPJ may be a regulating factor for PMT. Recently, it has been reported that GSCs with mesenchymal signatures were generated from GSCs with proneural signatures.[27] However, it is still uncertain whether GBMs initiate as proneural tumors and evolve to gain more mesenchymal phenotypes or that some GBMs initiate as mesenchymal tumors. The suppression of RBPJ caused a transition of phenotype from mesenchymal to proneural in GSCs, leading to slower tumor progression. Therefore, it is considered that inducing this kind of phenotype transition may also be an effective method to improve the prognosis of GBM patients. Some signaling pathways and factors are hijacked by GBM to regulate PMT, including STAT3, C/EBP, TAZ, NF-κB pathways and so on.[50,52] Administration of IL-6 could reverse the effect on PMT caused by RBPJ suppression, and indicated that RBPJ might regulate PMT through an IL-6-STAT3 pathway.

In conclusion, RBPJ can promote tumor progression in GSCs through activation of the IL-6/STAT3 pathway and PMT induction (Figure S10). Therefore, RBPJ is a promising therapeutic target for GBM. Our study provides an essential foundation for the development of RBPJ inhibitors for anti-GBM therapy.

ACKNOWLEDGMENTS

The authors are grateful to Erika Komura and Anri Machi for help with immunohistochemistry. This work was supported by JSPS KAKENHI (17K10858 to ST, 18H02910 to MN), a Kobayashi International Scholarship Foundation (to MN) and the China Scholarship Council (to GZ).

DISCLOSURES

No conflicts of interest are declared by the authors.

ORCID

Mitsutoshi Nakada https://orcid.org/0000-0001-9419-6101

REFERENCES

1. Ostrom QT, Gittleman H, Truitt G, Boscia A, Kruchko C, Barnholtz-Sloan JS. CBTRUS statistical report: primary brain and other central nervous system tumors diagnosed in the United States in 2011–2015. *Neuro Oncol*. 2018;20:iv1-iv86.
2. Lathia JD, Mack SC, Mulkearns-Hubert EE, Valentim CL, Rich JN. Cancer stem cells in glioblastoma. *Genes Dev*. 2015;29:1203-1217.
3. Singh SK, Clarke ID, Terasaki M, et al. Identification of a cancer stem cell in human brain tumors. *Cancer Res*. 2003;63:5821-5828.
4. Bao S, Wu Q, McLendon RE, et al. Glioma stem cells promote radioresistance by preferential activation of the DNA damage response. *Nature*. 2006;444:756-760.
5. Calabrese C, Poppleton H, Kocak M, et al. A perivascular niche for brain tumor stem cells. *Cancer Cell*. 2007;11:69-82.
6. Cheng L, Huang Z, Zhou W, et al. Glioblastoma stem cells generate vascular pericytes to support vessel function and tumor growth. *Cell*. 2013;153:139-152.
7. Gilbertson RJ, Rich JN. Making a tumour's bed: glioblastoma stem cells and the vascular niche. *Nat Rev Cancer*. 2007;7:733-736.
8. Singh SK, Hawkins C, Clarke ID, et al. Identification of human brain tumour initiating cells. *Nature*. 2004;432:396-401.
9. Louvi A, Artavanis-Tsakonas S. Notch signalling in vertebrate neural development. *Nat Rev Neurosci*. 2006;7:93-102.
10. Yoon K, Gaiano N. Notch signaling in the mammalian central nervous system: insights from mouse mutants. *Nat Neurosci*. 2005;8:709-715.
11. Kanamori M, Kawaguchi T, Nigro JM, et al. Contribution of Notch signaling activation to human glioblastoma multiforme. *J Neurosurg*. 2007;106:417-427.
12. Purow BW, Haque RM, Noel MW, et al. Expression of Notch-1 and its ligands, Delta-like-1 and Jagged-1, is critical for glioma cell survival and proliferation. *Cancer Res*. 2005;65:2353-2363.
13. Díaz-Trelles R, Scimia MC, Bushway P, et al. Notch-independent RBPJ controls angiogenesis in the adult heart. *Nat Commun*. 2016;7:12088.
14. Hori K, Cholewa-Waclaw J, Nakada Y, et al. A nonclassical bHLH Rbpj transcription factor complex is required for specification of GABAergic neurons independent of Notch signaling. *Genes Dev*. 2008;22:166-178.
15. Masui T, Long Q, Beres TM, Magnuson MA, MacDonald RJ. Early pancreatic development requires the vertebrate suppressor of hairless (RBPJ) in the PTF1 bHLH complex. *Genes Dev*. 2007;21:2629-2643.
16. Fan X, Matsui W, Khaki L, et al. Notch pathway inhibition depletes stem-like cells and blocks engraftment in embryonal brain tumors. *Cancer Res*. 2006;66:7445-7452.

17. Wang J, Sullenger BA, Rich JN. Notch signaling in cancer stem cells. In: Reichrath J, Reichrath S, eds. *Notch Signaling in Embryology and Cancer*. New York, NY: Springer, US; 2012:174-185.
18. Louis DN, Perry A, Reifenberger G, et al. The 2016 World Health Organization Classification of tumors of the central nervous system: a summary. *Acta Neuropathol*. 2016;131:803-820.
19. Dong YU, Furuta T, Sabit H, et al. Identification of antipsychotic drug fluspirilene as a potential anti-glioma stem cell drug. *Oncotarget*. 2017;8:111728-111741.
20. Nakada M, Niska JA, Miyamori H, et al. The phosphorylation of EphB2 receptor regulates migration and invasion of human glioma cells. *Cancer Res*. 2004;64:3179.
21. Tanaka S, Nakada M, Yamada D, et al. Strong therapeutic potential of γ-secretase inhibitor MRK003 for CD44-high and CD133-low glioblastoma initiating cells. *J Neurooncol*. 2015;121:239-250.
22. Tamase A, Muraguchi T, Naka K, et al. Identification of tumor-initiating cells in a highly aggressive brain tumor using promoter activity of nucleostemin. *Proc Natl Acad Sci*. 2009;106:17163.
23. Nair AK, Sutherland JR, Traurig M, et al. Functional and association analysis of an Amerindian-derived population-specific p.(Thr280Met) variant in RBPJL, a component of the PTF1 complex. *Eur J Hum Genet*. 2018;26:238-246.
24. Sun Z, Wang LI, Zhou Y, et al. Glioblastoma stem cell-derived exosomes enhance stemness and tumorigenicity of glioma cells by transferring Notch1 protein. *Cell Mol Neurobiol*. 2020;40(5):767-784.
25. Yu H, Lee H, Herrmann A, Buettner R, Jove R. Revisiting STAT3 signalling in cancer: new and unexpected biological functions. *Nat Rev Cancer*. 2014;14:736-746.
26. Phillips HS, Kharbanda S, Chen R, et al. Molecular subclasses of high-grade glioma predict prognosis, delineate a pattern of disease progression, and resemble stages in neurogenesis. *Cancer Cell*. 2006;9:157-173.
27. Ozawa T, Riester M, Cheng Y-K, et al. Most human non-GCIMP glioblastoma subtypes evolve from a common proneural-like precursor glioma. *Cancer Cell*. 2014;26:288-300.
28. Flavahan WA, Drier Y, Liau BB, et al. Insulator dysfunction and oncogene activation in IDH mutant gliomas. *Nature*. 2016;529:110-114.
29. Bi J, Chowdhry S, Wu S, Zhang W, Masui K, Mischel PS. Altered cellular metabolism in gliomas – an emerging landscape of actionable co-dependency targets. *Nat Rev Cancer*. 2020;20:57-70.
30. Xie QI, Wu Q, Kim L, et al. RBPJ maintains brain tumor-initiating cells through CDK9-mediated transcriptional elongation. *J Clin Investig*. 2016;126:2757-2772.
31. Maciaczyk D, Picard D, Zhao L, et al. CBF1 is clinically prognostic and serves as a target to block cellular invasion and chemoresistance of EMT-like glioblastoma cells. *Br J Cancer*. 2017;117:102-112.
32. Liu Y, Beyer A, Aebersold R. On the dependency of cellular protein levels on mRNA abundance. *Cell*. 2016;165:535-550.
33. Sivasankaran B, Degen M, Ghaffari A, et al. Tenascin-C is a novel RBPJkappa-induced target gene for Notch signaling in gliomas. *Cancer Res*. 2009;69:458-465.
34. Chen R, Nishimura MC, Bumbaca SM, et al. A hierarchy of self-renewing tumor-initiating cell types in glioblastoma. *Cancer Cell*. 2010;17:362-375.
35. Bayin NS, Frenster JD, Sen R, et al. Notch signaling regulates metabolic heterogeneity in glioblastoma stem cells. *Oncotarget*. 2017;8:64932-64953.
36. Piperi C, Papavassiliou KA, Papavassiliou AG. Pivotal role of STAT3 in shaping glioblastoma immune microenvironment. *Cells*. 2019;8(11):1398.
37. Stechishin OD, Luchman HA, Ruan Y, et al. On-target JAK2/STAT3 inhibition slows disease progression in orthotopic xenografts of human glioblastoma brain tumor stem cells. *Neuro Oncol*. 2013;15:198-207.
38. Han TJ, Cho BJ, Choi EJ, et al. Inhibition of STAT3 enhances the radiosensitizing effect of temozolomide in glioblastoma cells in vitro and in vivo. *J Neurooncol*. 2016;130:89-98.
39. Tan MSY, Sandanaraj E, Chong YK, et al. A STAT3-based gene signature stratifies glioma patients for targeted therapy. *Nat Commun*. 2019;10:3601.
40. Liu Q, Li G, Li R, et al. IL-6 promotion of glioblastoma cell invasion and angiogenesis in U251 and T98G cell lines. *J Neurooncol*. 2010;100:165-176.
41. Silva TCC, de Faria Lopes GP, de J. Menezes-Filho N, et al. Specific cytostatic and cytotoxic effect of dihydrochelerythrine in glioblastoma cells: role of NF-κB/β-catenin and STAT3/IL-6 pathways. *Anticancer Agents Med Chem*. 2018;18:1386-1393.
42. Kannabiran C, Zeng X, Vales LD. The mammalian transcriptional repressor RBP (CBF1) regulates interleukin-6 gene expression. *Mol Cell Biol*. 1997;17:1-9.
43. Vales LD, Friedl EM. Binding of C/EBP and RBP (CBF1) to overlapping sites regulates interleukin-6 gene expression. *J Biol Chem*. 2002;277:42438-42446.
44. Wongchana W, Palaga T. Direct regulation of interleukin-6 expression by Notch signaling in macrophages. *Cell Mol Immunol*. 2012;9:155-162.
45. Liau BB, Sievers C, Donohue LK, et al. Adaptive chromatin remodeling drives glioblastoma stem cell plasticity and drug tolerance. *Cell Stem Cell*. 2017;20:233-246.e237.
46. Rahaman SO, Harbor PC, Chernova O, Barnett GH, Vogelbaum MA, Haque SJ. Inhibition of constitutively active Stat3 suppresses proliferation and induces apoptosis in glioblastoma multiforme cells. *Oncogene*. 2002;21:8404-8413.
47. Verhaak RGW, Hoadley KA, Purdom E, et al. Integrated genomic analysis identifies clinically relevant subtypes of glioblastoma characterized by abnormalities in PDGFRA, IDH1, EGFR, and NF1. *Cancer Cell*. 2010;17:98-110.
48. Behnan J, Finocchiaro G, Hanna G. The landscape of the mesenchymal signature in brain tumours. *Brain*. 2019;142:847-866.
49. Bhat K, Balasubramaniyan V, Vaillant B, et al. Mesenchymal differentiation mediated by NF-κB promotes radiation resistance in glioblastoma. *Cancer Cell*. 2013;24:331-346.
50. Kim S-H, Ezhilarasan R, Phillips E, et al. Serine/threonine kinase MLK4 determines mesenchymal identity in glioma stem cells in an NF-κB-dependent manner. *Cancer Cell*. 2016;29:201-213.
51. Mao P, Joshi K, Li J, et al. Mesenchymal glioma stem cells are maintained by activated glycolytic metabolism involving aldehyde dehydrogenase 1A3. *Proc Natl Acad Sci*. 2013;110(21):8644-8649.
52. Fedele M, Cerchia L, Pegoraro S, Sgarra R, Manfioletti G. Proneural-mesenchymal transition: phenotypic plasticity to acquire multitherapy resistance in glioblastoma. *Int J Mol Sci*. 2019;20(11):2746.

SUPPORTING INFORMATION

Additional supporting information may be found online in the Supporting Information section.

How to cite this article: Zhang G, Tanaka S, Jiapaer S, et al. RBPJ contributes to the malignancy of glioblastoma and induction of proneural-mesenchymal transition via IL-6-STAT3 pathway. *Cancer Sci*2020;111:4166–4176. https://doi.org/10.1111/cas.14642